

Anatomical Markers for the Subdivisions of the Barn Owl's Inferior-Collicular Complex and Adjacent Peri- and Subventricular Structures

HERMANN WAGNER,^{1*} ONUR GÜNTÜRKÜN,² AND BÄRBEL NIEDER¹

¹Institut für Biologie II, Rheinisch Westfälische Technische Hochschule Aachen, D-52074 Aachen, Germany

²Arbeitseinheit Biopsychologie, Ruhr-Universität Bochum, D-44780 Bochum, Germany

ABSTRACT

The anatomy of the inferior-collicular complex of the barn owl, situated below the fourth ventricle in the tectal lobe, was studied by determining the distribution of antigens with antibodies directed against tyrosine hydroxylase, γ -aminobutyric acid (GABA)_{AB}, dopamine- and cyclic AMP-regulated phosphoprotein (DARPP-32), calretinin, and calbindin. Additionally, the somata were stained with cresyl violet, and fibers were marked according to the Gallyas procedure. These markers were chosen to allow for an easy delineation of the boundaries between the subnuclei of the inferior colliculus. We could discriminate eight structures that belong to the three subnuclei of the inferior colliculus [the central nucleus (ICC), the superficial nucleus (ICS), the external nucleus (ICX)] and to the optic tectum. Periventricular tectal layers 15a and 15b stained well with all the antibodies used. The ICS, embedded in tectal layer 15a, may be divided into a dorsal and a ventral lamina. It does not have direct contact with the other nuclei of the inferior colliculus. The border between tectal layer 15a and ICX was well marked by all antibodies, but less so in Gallyas and cresyl violet stains. The ICC consists of a core and a medial and lateral shell. The core was clearly demarcated with antibodies against calretinin and calbindin. The border between the lateral shell and the ICX was marked less well than the borders between ICX and 15a, but the somata were much more darkly labeled with the DARPP-32 antibody in ICX than in the lateral shell of ICC. None of the markers delineated the border between the medial and lateral shell of ICC. *J. Comp. Neurol.* 465:145–159, 2003. © 2003 Wiley-Liss, Inc.

Indexing terms: space map; superior colliculus; auditory system; external nucleus

The auditory midbrain in birds forms the dorsal part of the torus semicircularis and has been termed nucleus mesencephalicus lateralis, pars dorsalis (MLd) (Karten, 1967). Because this formation is believed to be homologous to the mammalian inferior colliculus (IC) (Karten, 1967), Knudsen (1983) recommended that the term IC be applied to refer to the MLd in birds. This terminology has been used in owl studies ever since and will be adopted here.

The avian as well as mammalian IC may be divided into three major subdivisions: the central (ICC), the external (ICX), and the superficial nuclei (ICS) (Rockel and Jones, 1973a,b; Knudsen, 1983; Morest and Oliver, 1984; Oliver and Shneiderman, 1991; Puelles et al., 1994; Wild, 1995). Based on its input patterns, the ICC in the barn owl ("owl") can be subdivided into a core (ICCs) and a shell (ICCs) (Takahashi and Konishi, 1988; Takahashi et al., 1989; Adolphs, 1993), with the shell containing a medial

and a lateral part (Takahashi et al., 1989; Adolphs, 1993; Kubke et al., 1999). Although much new information has come to light since the influential paper by Knudsen (1983), a thorough revision of the anatomy of the owl IC and its relation to the mammalian and general avian IC is lacking. The ICS, for example, first mentioned by Knudsen (1983), has not been described further since then.

Grant sponsor: the Deutsche Forschungsgemeinschaft; Grant number: Wa-606/1001 (H.W.); Grant number: Di459/2-3 (O.G.).

*Correspondence to: Hermann Wagner, Institut für Biologie II, RWTH Aachen, Kopernikusstrasse 16, D-52074 Aachen, Germany. E-mail: wagner@bio2.rwth-aachen.de

Received 23 July 2002; Revised 12 March 2003; Accepted 7 May 2003
DOI 10.1002/cne.10826

Published online the week of August 18, 2003 in Wiley InterScience (www.interscience.wiley.com).

The IC plays an important role in the processing of sound-source location. More specifically, the ICX, which lies lateral to the ICC, contains a map of auditory space (Knudsen and Konishi, 1978). This map is assembled in the ICCs and the ICX (Mazer, 1998) and is projected topographically from the ICX to the optic tectum (OT) (Knudsen and Knudsen, 1983; Hyde and Knudsen, 2000). Experiments on developmental plasticity demonstrated visual calibration of the auditory map of space. Map shifts induced by prism-rearing were absent in ICCs and maximal in the lateral division of the ICX (Brainard and Knudsen, 1993; Feldman and Knudsen, 1997; Gold and Knudsen, 2000; deBello et al. 2001). Only the shift observed in the lateral part of the ICX was large enough to account for the shift measured in the OT, suggesting a division of the ICX into a medial and lateral part (Brainard and Knudsen, 1993). A recently reported projection from the optic tectum to the ICX may be a putative correlate that could induce such a shift (Luksch et al., 2000; Hyde and Knudsen, 2000).

The anatomy and connectivity as well as the functional role of the ICX has been a source of debate ever since the space map was first described in the owl, as this structure, in addition to its auditory function (e.g., Aitkin et al., 1985; Binns et al., 1992), is known to receive somatosensory input in mammals (Atkin et al., 1978).

Using contemporary antibodies, we undertook a thorough anatomical investigation of the IC complex with the objective of delineating the boundaries of the subnuclei more thoroughly than was previously possible. This helped us to tackle the three questions raised in the last three paragraphs, namely, the nature of the ICS, the anatomical correlates of developmental plasticity, and the similarities and differences between the owl IC and the IC in other birds and in mammals.

MATERIALS AND METHODS

Stainings of brain sections were obtained from eight adult barn owls (*Tyto alba*). In six animals coronal sections throughout the anteroposterior extent were processed. In addition, the brain was divided mediosagittally in two owls; then one hemisphere was cut horizontally,

and the other was cut coronally. As we did not observe differences between individual owls, we display data from only one bird for which we have material from both coronal and horizontal sections.

Barn owls were anesthetized with ketamine (15–20 mg/kg IM) followed by an overdose of pentobarbital (35 mg/kg IM). After intracardiac injection of heparin, barn owls were perfused with saline, followed by either 4% paraformaldehyde or 2% paraformaldehyde and 2.5% glutaraldehyde in 0.1 M phosphate buffer (pH 7.4; PB). The brains were postfixed in the perfusion solution for varying lengths of time, and then cryoprotected in 30% sucrose in PB at 4°C. Good histological preservation was achieved without a marked loss of antigenicity using these fixatives or after prolonged periods of postfixation. The brains were sectioned on a freezing microtome at 30 µm thickness, and the sections were collected in PB. All procedures were approved by German authorities (Regierungspraesidium Tuebingen and Regierungspraesidium Koeln) and conformed to NIH guidelines.

The distributions of various antigens in the IC complex were determined by using antibodies directed against: 1) tyrosine hydroxylase (TH; Chemicon, Temecula, CA; cat. No. MAB358), the rate-limiting enzyme of catecholaminergic synthesis; 2) GABA_{Aβ} (Boehringer, Mannheim, Germany; anti-GABA_A receptor, β-chain; clone bd17; cat. no. 1381 458); 3) DARPP-32 (kindly provided by H. C. Hemmings, Jr., Cornell University, Ithaca, NY), a dopamine- and cyclic AMP-regulated phosphoprotein of M_r 32,000 that is closely associated with cells expressing the dopamine D1-receptor (Ouimet et al., 1984; Hemmings et al., 1987); 4) calretinin (Swant, Bellinzona, Switzerland; cat. no. 7696); and 5) calbindin (7E4 F2, kindly provided by C.E. Carr).

Standard immunohistochemical procedures were followed using the avidin-biotin-peroxidase complex (ABC) method with reagents from Vectastain elite kits (Vector, Burlingame, CA).

For calretinin (CR) immunocytochemistry, sections were preincubated for 1 hour in 0.5 M Tris-HCl buffer (pH 7.6) with 4% normal serum and 0.4% Triton X-100. They were then incubated overnight in the primary antibody (1:1,000). Floating sections were incubated for 10 minutes in 3% H₂O₂ in Tris-HCl, washed, incubated for 1 hour in the diluted biotinylated secondary antibody, washed, incubated in ABC for 1 hour, washed, incubated in secondary antibody for 1 hour, washed, incubated in ABC for 1 hour, and then washed for 20 minutes in Tris-HCl followed by 20 minutes in chromogen buffer. Sections were treated with diaminobenzidine tetrahydrochloride (DAB, 0.48 mg/ml) and 0.03% H₂O₂ in Tris-imidazole buffer (pH 6.5). Nickel sulfate intensification was used in most cases. Sections were incubated with nickel sulfate (26.3 mg/ml) in acetate imidazole buffer (pH 6.5). Sections were mounted onto subbed slides, dehydrated, cleared, and coverslipped with Permount. Some sections were additionally counterstained with neutral red.

For staining against TH, DARPP-32, calbindin, and GABA_{Aβ} free-floating sections were incubated in the primary antisera (TH 1:200, GABA_{Aβ} 1:100, DARPP-32 1:10,000, calbindin 1:5,000). Sections were washed three times in PB for a total of 30 minutes and incubated for an additional 30 minutes at room temperature in 10% serum of the same species of animal in which the secondary antibody was raised. The sections were washed again for

Abbreviations

15a, 15b	sublayers of layer 15 of optic tectum
DARPP-32	dopamine- and cyclic AMP-regulated phosphoprotein
GABA	γ-aminobutyric acid
IC	inferior colliculus
ICC	central nucleus of inferior colliculus
ICCc	core of the central nucleus of the inferior colliculus
ICCs	shell of the central nucleus of the inferior colliculus
ICCsms	medial shell of the central nucleus of the inferior colliculus
ICCl	lateral shell of the central nucleus of the inferior colliculus
ICS	superficial nucleus of inferior colliculus
ICSd	dorsal part of ICS
ICSv	ventral part of ICS
ICX	external nucleus of inferior colliculus
IR	immunoreactivity
MLd	nucleus mesencephalicus lateralis, pars dorsalis
OT	optic tectum
PB	phosphate buffer
TH	tyrosine hydroxylase
V	ventricle

10 minutes in PB and then incubated in the diluted biotinylated secondary antibody in 0.3% Triton X-100 for 1 hour at room temperature. The tissue was then washed three times in PB for 10 minutes each and incubated for 1 hour in ABC, diluted 1:100 in Triton X-100 at room temperature. Following three washes in PB for 10 minutes each, the sections were incubated with 0.05% DAB in PB for 15 minutes. Hydrogen peroxidase was added to the incubation medium to make a final concentration of 0.01%, and the dish was gently shaken as the reaction proceeded. After 20 minutes, the reaction was stopped with several washes of PB. Sections were mounted on gelatin-coated slides and dried. Afterward the DAB reaction product was intensified by immersing the sections in 0.1% osmium tetroxide in PB for 30 seconds. After a final buffer wash, the sections were cleared and coverslipped.

For DAB labeling of DARPP-32 sections, 400 mg/100 ml β -D-glucose were added to the solution. After 15 minutes of preincubation, the reaction was catalyzed with 100–200 U/mg glucose-oxidase (type VII, Sigma, St. Louis, MO). In some cases, a solution of 0.3% H_2O_2 was used to catalyze the reaction instead of β -D-glucose and glucose-oxidase. Finally, slices were washed three more times for 5 minutes in 0.12 M acetate buffer and two times in PB.

Two different controls were conducted to demonstrate the specificity of the immunocytochemical staining pattern. As a first control, a complete staining sequence was run without prior incubation in any primary antibody. In this case, the staining was completely abolished. As a more specific control, the antibody against TH was incubated with 10^{-5} M of the appropriate antigens for 12 hours at 4°C before application onto the sections. In these cases the sections were either completely blank or displayed only an extremely light brown and nonspecific background. Because $GABA_{A\beta}$ could not be purchased as an antigen, this type of control could not be performed. The specificity of the antibodies directed against DARPP-32 and calretinin was assessed by immunoblotting (Durstewitz et al. 1998, Schwaller et al. 1993).

One of six sections was stained with cresyl violet to allow correlations of immunohistochemical findings with traditional cytoarchitectonic subdivisions. A further parallel series of sections was stained according to the Gallay procedure (Hess and Merker, 1983).

Analysis

Analyses were carried out on sections cut in both the transverse and horizontal planes. The distribution of the various staining patterns was mapped onto drawings of the IC complex. For this purpose, video images of calretinin-stained reference sections were captured with a digital camera and imported into a graphics program (CorelDraw). Then the outlines of the midbrain and of clearly definable structures such as the ventricle, the outline of the OT, etc. were drawn at intervals of 360 μ m. Sections from the same animal stained for the visualization of different antigens were then imaged onto these preliminary maps. Clearly visible cell groups and fiber tracts were drawn. In a third step, fine details of the immunocytochemical staining were added with microscopic inspections of the sections. Digital images were adjusted for brightness and contrast (Corel PhotoPaint).

RESULTS

In the barn owl, the optic lobe is situated parallel to the ventral border of the telencephalon. The optic lobe has an oval shape with an extended anterior-posterior axis (s. inset in Fig. 1).

The frontal sections shown here were cut perpendicular to the anterior-posterior axis of the optic lobe. The sections are named Ax, with $x = 0$ being the caudal pole of the optic tectum. The horizontal sections were cut perpendicular to the dorsoventral axis. The sections are named Dy, with $y = 0$ corresponding to the ventral end of the fourth ventricle. The two most conspicuous structures within the optic lobe are the optic tectum that surrounds the ventricle, and the inferior colliculus lying below and medial to the ventricle (Fig. 1, A3.82). The inferior colliculus is part of the subventricular complex, which also includes the tectal layer 15 and the intercollicular nuclei. All of these components can be divided further.

In the subsequent paragraphs a description of the general anatomy will be provided followed by a more detailed sketch of the substructures of the IC complex as well as the adjacent tectal layer 15.

General anatomy

The lateral and dorsal borders of the IC complex lie close to the ventricle whereas the ventral and medial borders are demarcated by fiber tracts [Fig. 1 (overview at 3.82), Figs. 5a, 6a, 7a, 8a,b, 9a, 10a]. At its frontal end, the tectal layer 15 has the shape of an ovoid body in frontal sections and is oriented at about 20 degrees to a line that is perpendicular to the midline of the brain (Figs. 1, A4.90, A4.54, 2). At this level the lateral part reaches down more ventrally than the medial part. Further posterior, as the IC complex appears and becomes larger, the ventral side bulges out and the medial border becomes more inclined relative to the midline of the brain (Fig. 1, A3.46 and further posterior). The IC complex gradually becomes more circular at the caudal end. At its widest margins, the IC complex extends approximately 3.5 mm mediolaterally, and 2.5–3 mm dorsoventrally. The anterior-posterior extent is about 4.5 mm.

On horizontal sections the IC complex and tectal layer 15 appear together dorsally with the outline of the fourth ventricle, which forms a circle at the dorsal edge (not shown). The ventricle extends about 2.5 mm ventrally and ends some 300 μ m before the ventral end of the IC. Because the most interesting borders are found in the ventral third of the nucleus, Figures 5b, 6d, 7c, 8g,h, 9d, and 10c were taken from this region.

On the basis of cyto- and fiberarchitectonic as well as immunocytochemical data, the IC complex can be divided into several components (Fig. 1). We begin with these schemes to simplify the understanding of the evidence presented subsequently. Beginning with a section from the middle of the IC complex at level A2.72, eight distinct structures could be identified (Fig. 1). In the center of the IC complex lies the core of the central nucleus of the IC (ICCc), which has the shape of an ellipse. In this section, the ICCc touches the ventral border of the IC and almost extends dorsally to the ventricle. At its medial edge, the ICCc shares a border with the medial shell of the ICC (ICCs). At its lateral side the ICCc adjoins the lateral shell of the ICC (ICCl). Together these three subnuclei form the central nucleus of the inferior colliculus (ICC). At

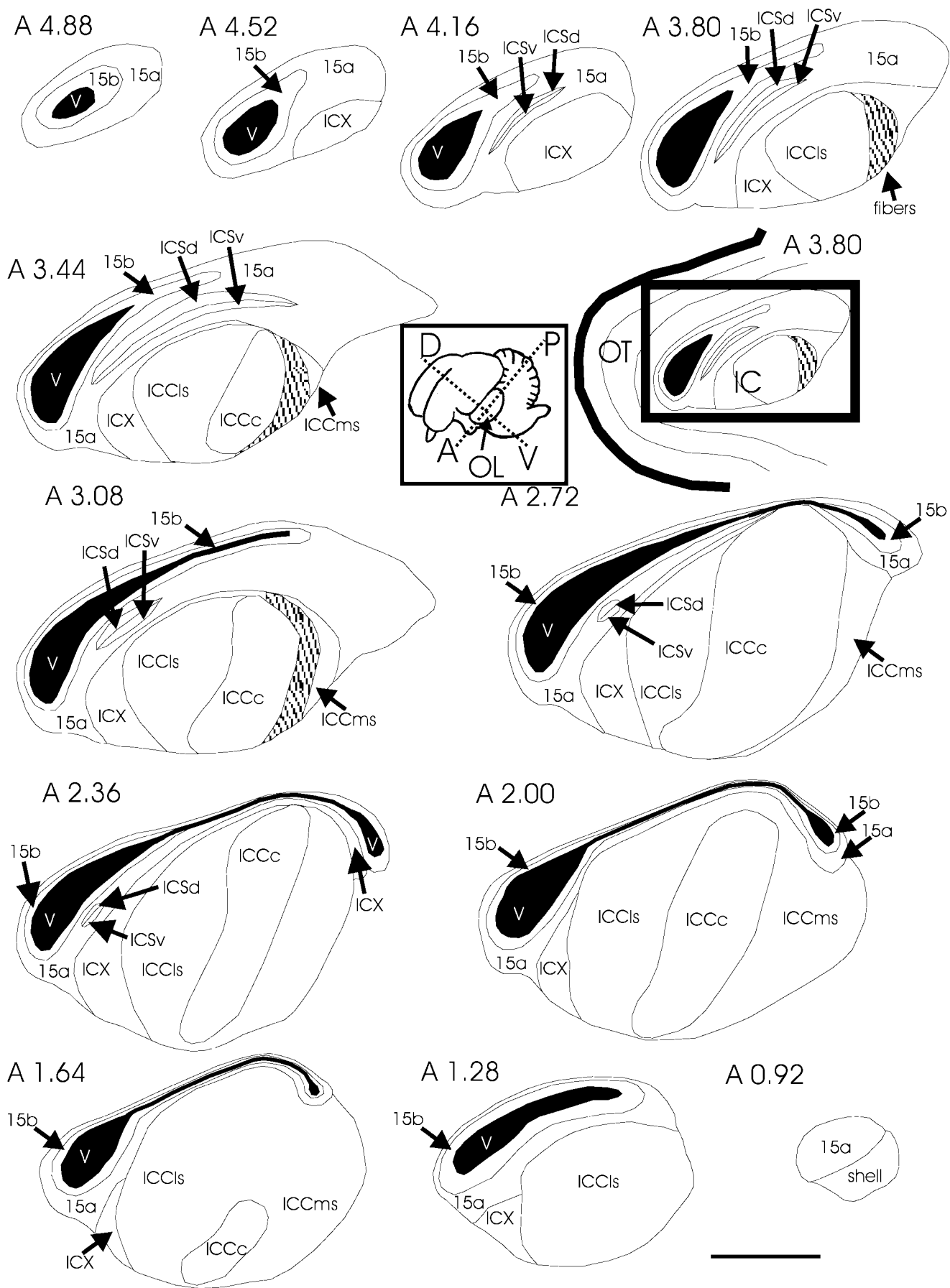


Figure 1

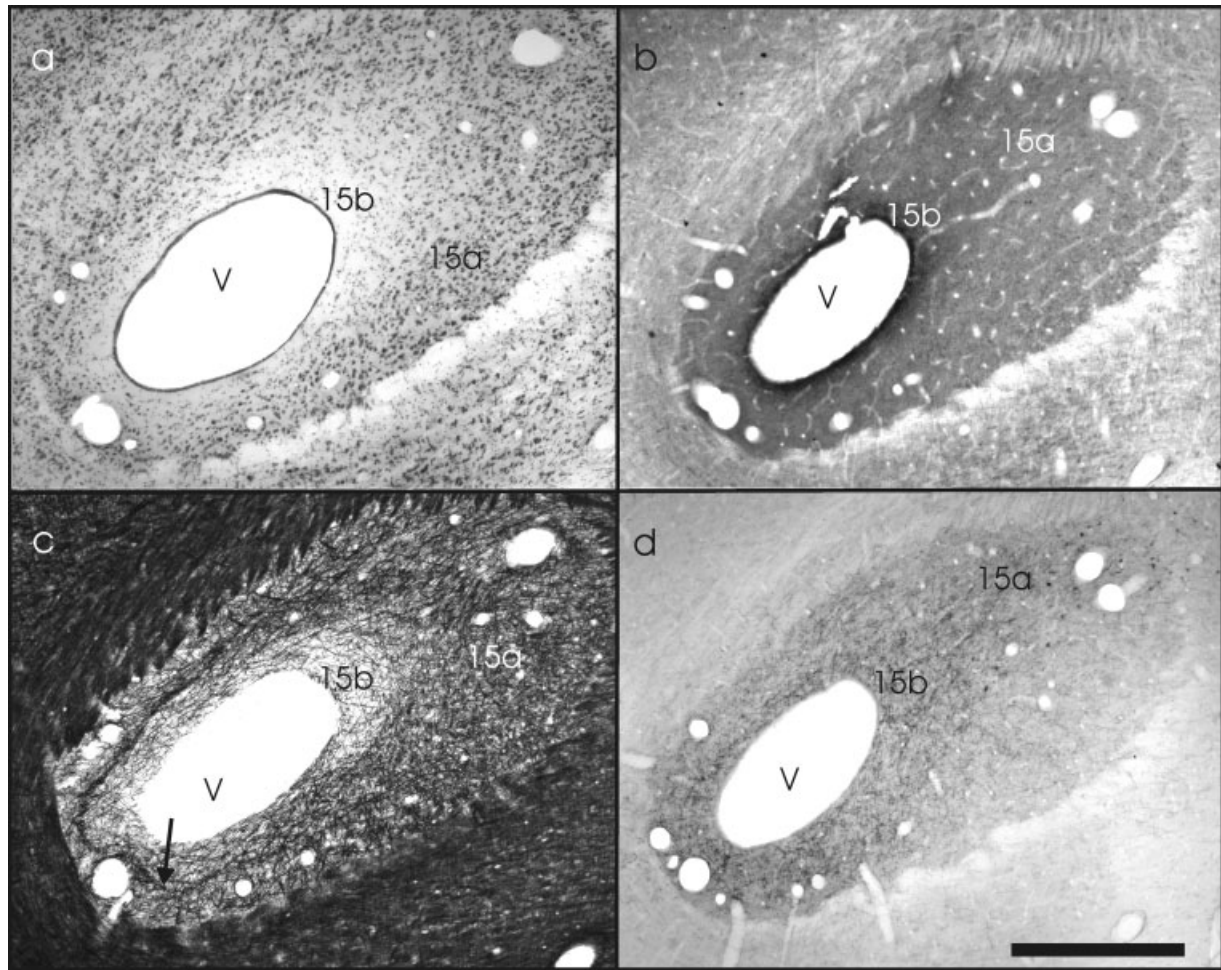


Fig. 2. Frontal sections from the anterior end of the IC complex shows laminae 15a and 15b at about A 4.52. **a:** Cresyl violet stain. **b:** GABA_{A β} -like labeling. **c:** Gallyas-stained fibers. **d:** TH-like labeling. Lateral is to the left, and dorsal is up. For abbreviations, see list. Scale bar = 500 μ m.

the lateral border of the ICC, another subnucleus can be distinguished by its staining pattern, the external nucleus of the IC (ICX). The ICX borders laterally at layer 15a of the optic tectum. In the middle of the IC, from A3.82 to A2.00, the ICX forms a thin dorsal rim around the ICC that may reach the medial border of the IC in some cases (A 2.36; Fig. 1).

Dorsal to the IC, four structures run parallel to the ventricle from dorsomedial to ventrolateral (Fig. 1, A

3.46). Two of the structures are part of tectal layer 15 as they surround the ventricle (Fig. 1) and the other two structures form the superficial nucleus of the IC (ICS).

Subcomponents

Tectal layer 15. Originally, Ramón y Cajal (1891) did not further subdivide this lamina. Later, a division of this layer into 15a and 15b was introduced by Cowan et al. (1961). Because a clear separation is present in our data (Figs. 2–10), we use the latter nomenclature. Layer 15a in the present study corresponds to the stratum griseum periventriculare whereas layer 15b constitutes the stratum album periventriculare of Karten (1967). Layer 15 begins anterior to the ventricle and disappears just after the caudal end of the ventricle, wrapping itself around the ventricle like a sheet.

The sublayers 15a and 15b may be distinguished in most stainings. From level A 3.46 to almost the caudal end of IC, layer 15 displayed a characteristic triangle-shaped widening at the ventrolateral end of the tectal ventricle (Fig. 1).

Fig. 1. Schematic overview in frontal plane of the various subdivisions of the inferior collicular complex in the barn owl. The inset shows the owl brain as seen from the side. The anterior (A)-posterior (P) as well as the dorso (D)-ventral (V) axes of the optic lobe (OL) are indicated. The second inset to the right of the A 3.46 plane provides an overview of the location of the structures at this location within the optic lobe. In the other drawings, the surrounding tectal laminae beyond layer 15 are not depicted. The numbers at the top left of each drawing refer to the distance in millimeters to the caudal pole of the optic tectum. Dorsal is up, and lateral is to the left. For abbreviations, see list. Scale bar = 1 mm.

In cresyl violet-stained sections, cells of layer 15a were highly basophilic, with round to oval perikarya that surrounded the ventricle in several sheets (Fig. 2a). In Gallyas-stained sections, layer 15 was mostly clear, with fibers scattered around the 15a/15b border (Figs. 2c, 6b). GABA_{Aβ} neuropil staining showed a moderate density throughout layer 15a (Figs. 2b, 9). TH staining was also moderate but denser in the frontal than in the caudal part and was restricted to the ventral part of layer 15 caudally (Fig. 10). Moderate staining in layer 15a was also observed with DARPP-32 (Fig. 7), calretinin (Fig. 8b,d,h), and calbindin (Fig. 8a,c,g). Somata were stained by the antibodies against DARPP-32 (Fig. 7b), calretinin (Fig. 8d), and calbindin (Fig. 8c). Very few cells were observed in TH stains (Fig. 10c). No GABA_{Aβ}-positive somata were present (Figs. 2b, 9b).

As mentioned before, the transition from 15a to 15b was demarcated as a thin line of fibers in Gallyas stains (Figs. 2c, 6b). Using this fiber border as a guideline, both layers could be followed around the ventricle. In cresyl violet-stained sections many glial elements, recognizable by their small size (Fig. 2a), were observed. Lamina 15b displayed an intense neuropil staining pattern with all immunohistochemical markers (Figs. 2b,d, 7–10).

ICS. The ICS has until now not been described in detail. It is embedded in layer 15a and first visible around A4.18 as a thin neuronal sheet. More posteriorly, the ICS increases rapidly in its mediolateral aspect and then shrinks again (Fig. 1: compare A4.18 with A3.46 and A2.72; Figs. 3, 4). The area of the ICS is largest around A 3.46 where it runs as a thin stripe for about 2.5 mm from ventrolateral to dorsomedial (Figs. 1, 4). More caudally the ICS takes on a bean-shaped appearance (Figs. 1, A2.72, 3). In horizontal sections the ICS appears as a thick arched line (Figs. 5b, 6d, 7c, 9d).

The ICS could be clearly differentiated in Gallyas, DARPP-32, GABA_{Aβ}, and calbindin stains. The nucleus was less visible in cresyl violet and calretinin stains. In stains with the antibody against TH, the ICS could not be detected. In Gallyas stains, the ICS could easily be differentiated from the surrounding layer 15a by the lower density of fibers and especially from the lack of mediolaterally oriented fibers (Figs. 3a, 4a, 6a). DARPP-32 labeled many ICS somata well within a lightly stained neuropil (Figs. 3b, 4b, 7a,c), allowing for a clear delineation of ICS within the lightly stained layer 15a. In contrast, in GABA_{Aβ} stains, the neuropil within the ICS showed darker label than the neuropil of the surrounding layer 15a, but no labeled somata were observed (Figs. 3c, 9a). Although these molecules were distributed over the total dorsoventral and mediolateral extent of the ICS, calbindin-labeled somata and neuropil were found only in the ventral part of the nucleus. A clear zone free of any stain characterized the dorsal ICS (Figs. 3d, 4c), suggesting a division of this nucleus into a dorsal and ventral part. This picture was altered when the calretinin antibody was used for labeling. With this antibody, neuropil staining was dense in both the ventral and dorsal part of the ICS, but many more somata were stained in the ventral than the dorsal part of the ICS (Fig. 3e).

ICX. The ICX-15a border was clearly demarcated in the immunocytochemical stains [DARPP-32 (Fig. 7), calbindin (Figs. 3d, 4c, 8a,c), GABA_{Aβ} (Fig. 9a,b,d), and TH (Fig. 10)], with some restrictions with respect to calretinin

(Fig. 8b,d,f,h), but less well in Gallyas (Fig. 6) and cresyl violet stains (Fig. 5).

The medial border of the ICX, the border to the ICCLs, was not as crisply demarcated as the lateral border. Nevertheless, DARPP-32 (Fig. 7), calbindin (Fig. 8c), GABA_{Aβ} (Fig. 9a,b,d), and Gallyas (Fig. 6a,c) stains allowed for a separation of the ICX from the ICCLs. Specifically, somata in the ICX were darkly labeled with DARPP-32, whereas in the ICCLs they were only moderately labeled (Fig. 7b). From these data, it appeared that the ICX extended to the medial border of the IC complex in the frontal part of the nucleus (Fig. 1, A4.54, A.4.18). However, through most of its length, the ICX formed a river-like stretch in the lateral portion of the IC complex that widened ventrally like an estuary (e.g., Fig. 7b).

When compared with neurons in the ICC, the cells in the ICX were smaller and less basophilic. The ICX was also characterized by a lower density of fibers and a more interwoven appearance of those fibers in Gallyas stains than in the ICC (Fig. 6a,c). The neuropil in the ICX exhibited a denser DARPP-32-like immunoreactivity (IR) than in layer 15 (Fig. 7). Calretinin-like IR was moderate in the neuropil, with highly stained somata scattered throughout the nucleus (Figs. 8d). The antibody against GABA_{Aβ} labeled the neuropil strongly and more densely than that of the laterally located triangular widening of layer 15a (Fig. 9). Neither neuropil nor somata showed TH-like immunoreactivity (Fig. 10).

ICC. The ICC of barn owls is by far the largest structure within the IC complex. The size of the ICC is enormous, especially in the middle of the anterior-posterior extent of the IC (Figs. 1, 5–10). We first describe the general staining properties in the ICC and then turn to the subdivisions of the nucleus, the central core (ICCc) and the surrounding shell (ICCs), which in itself may be divided into a lateral (ICCLs) and a medial part (ICCMs).

The ICC does not reach the frontalmost end of the IC complex but lies behind the ICX, where this nucleus reaches the medial edge of the IC (Fig. 1, A4.18). The ICC first appears at around A3.82 and quickly increases in size, occupying much more than 50% of the IC complex area in its middle and caudal part.

Due to the presence of layer 15 below the ventricle, ICC was not observed to have contact with the ventricular ependymal layer. However, the ICC was so large at more caudal levels that it came very close to the ventricle, compressing neurons and fibers of layers 15a and 15b into a single thin layer (Fig. 1, A2.72). As the ICC starts to extend more toward the ventricle in the caudal part of the IC complex, the medial extension of the ICS disappears (compare Fig. 1 A3.46 with A2.72).

In Gallyas preparations the ICC was easily recognizable by its dense fiber structure (Fig. 6a,c,d). More specifically, a thick fiber track was running dorsoventrally close to the medial edge (Fig. 6a) that caused a lightening of the stain with DARPP-32 (Fig. 7a) and GABA_{Aβ} (Fig. 9a) in this region. Apart from the region of the fiber tract, the antibody against GABA_{Aβ} labeled all regions of the ICC in a similar fashion. It also caused a moderate staining of neuropil (Fig. 9). A moderate number of somata were surrounded by GABA_{Aβ}-like immunoreactive terminals (Fig. 9c) allowing for a clear distinction from the more uniform and darker neuropil staining in the ICX that was also free of soma labeling with the antibody against

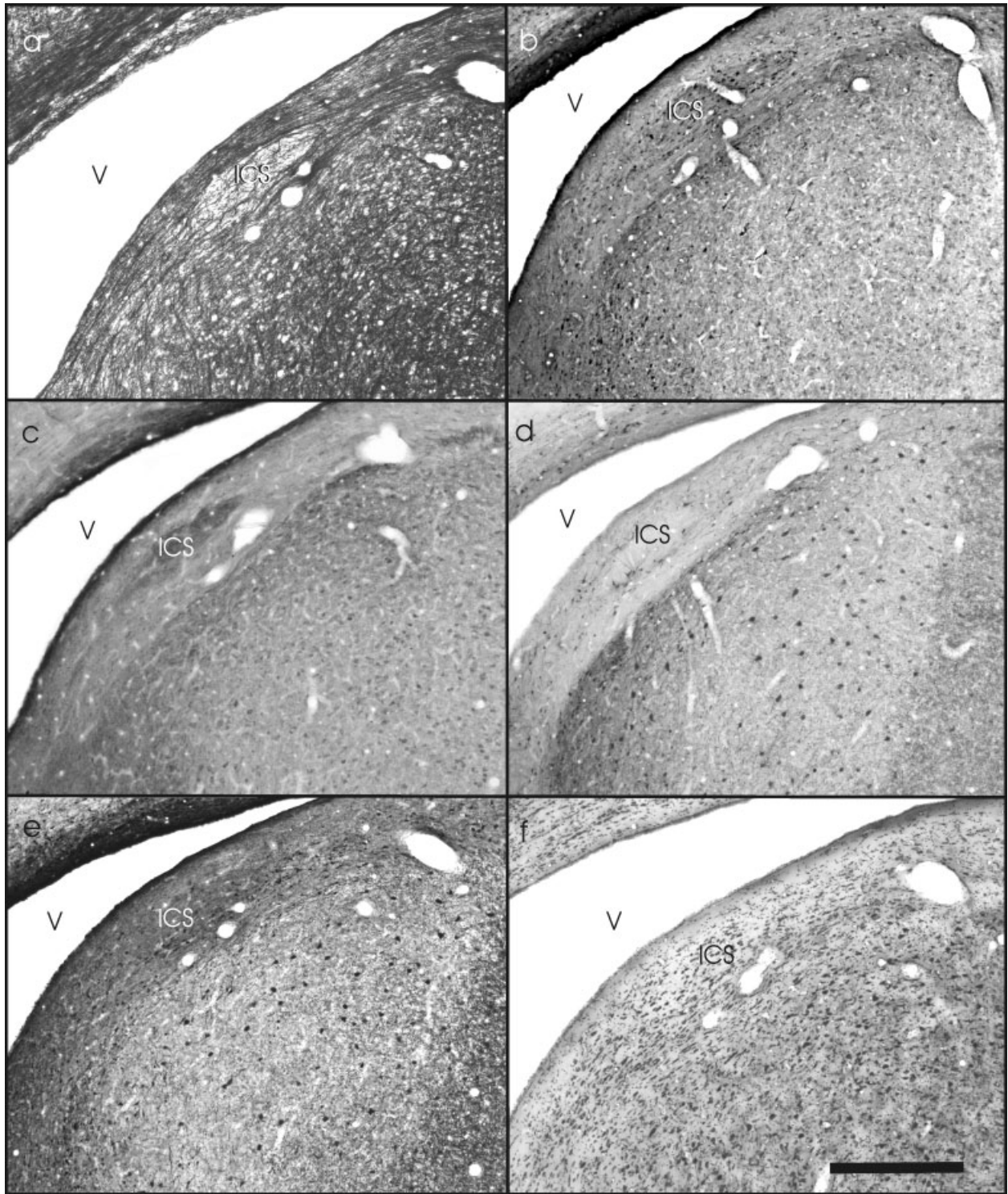


Fig. 3. Delineation and staining of ICS. **a:** Gallyas stain from A 3.05. ICS is the lightly stained bean-shaped region below the ventricle. **b:** DARPP-32 stain from A 3.14. **c:** $GABA_{A\beta}$ from A2.99. **d:** Calbindin stain from A3.17. **e:** Calretinin stain from A3.08. **f:** Cresyl violet stain from A3.02. Note that calbindin stains only the ventral part of ICS. For abbreviations, see list. Scale bar = 500 μ m.

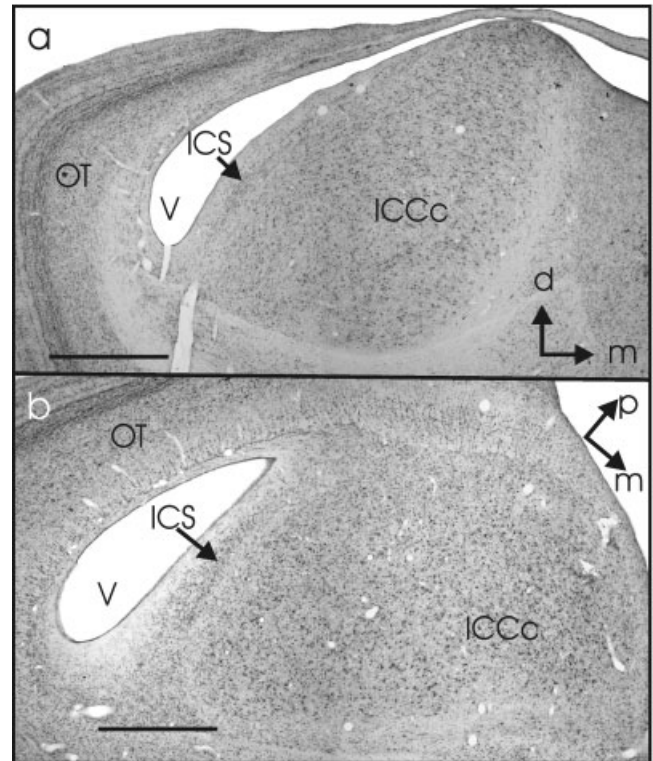
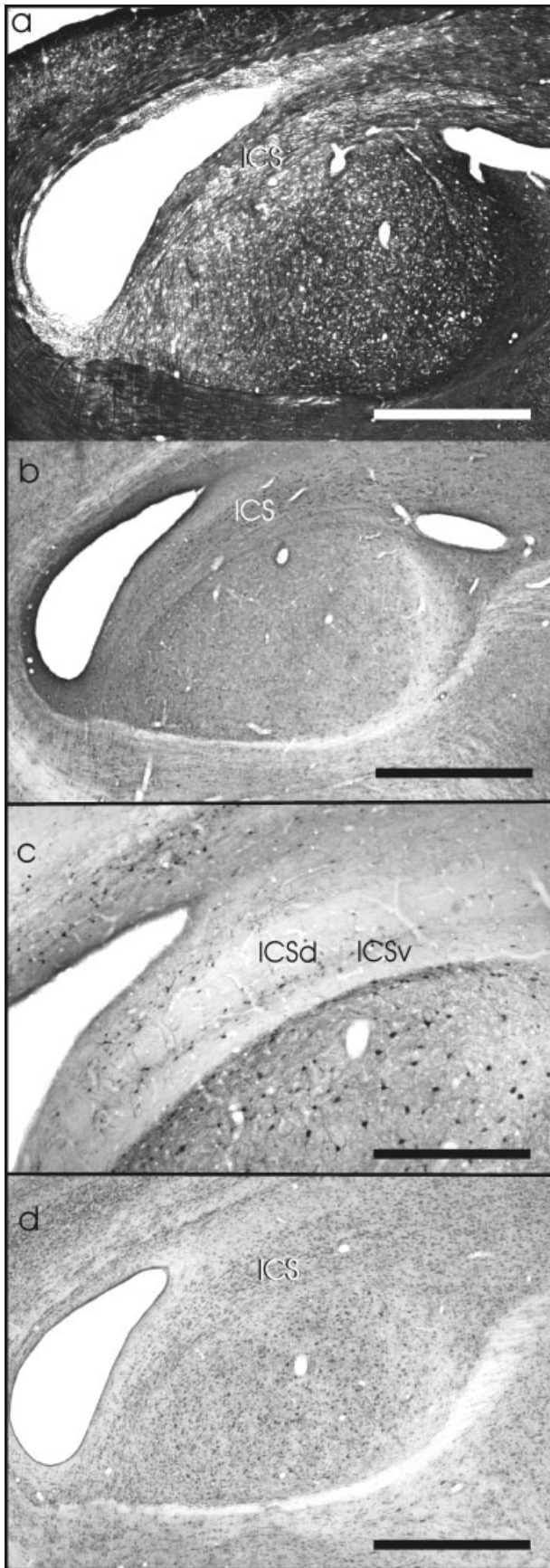
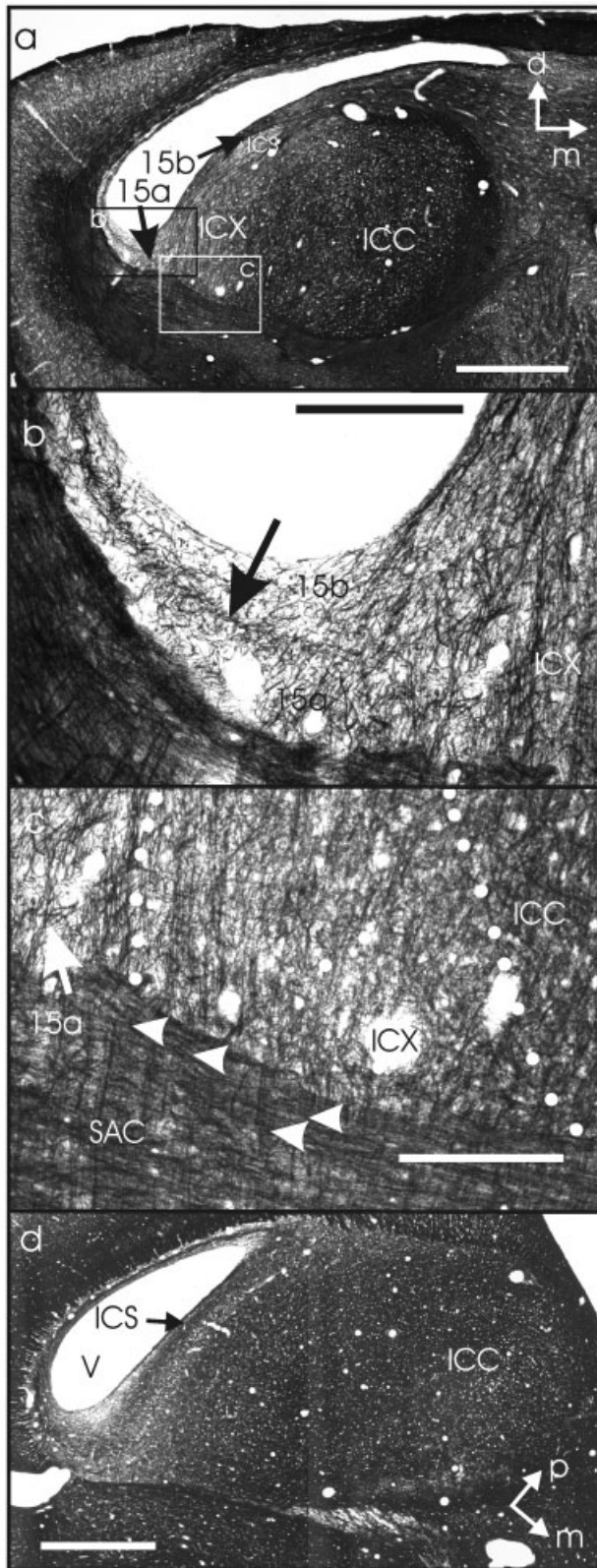


Fig. 5. Cresyl violet-stained sections providing an overview over the inferior-collicular complex. **a:** Frontal section from A3.11. **b:** Horizontal section from the lower third of the nucleus (D 0.63). p, posterior; m, medial; d, dorsal. For other abbreviations, see list. Scale bars = 1,000 μm .

GABA_{A β} . Only a very faint label was seen in the ICC with TH stains.

Although these stains labeled ICC rather uniformly, the subnuclei became apparent by staining against calretinin, calbindin, and cresyl violet, as reported earlier (Takahashi et al. 1987, Feldman and Knudsen 1997, Kubke et al. 1999). The antibodies against calbindin and calretinin stained the neuropil of ICCc darkly with scattered immunopositive somata. The surrounding ICCs showed a much lighter staining of the neuropil (Fig. 8), with some highly stained scattered somata. Calbindin and calretinin stains were slightly different, with calbindin exhibiting clearer borders than calretinin (compare Fig. 8a,c,e,g with 8b,d,f,h). The ICCc was also visible, albeit only faintly, in DARPP-32 stains. Here, the neuropil of the ICCc stained slightly lighter than the neuropil of the ICCl. Somata were stained moderately throughout the ICC (Fig. 7). In cresyl violet stains the ICCc appeared as a distinct cytoarchitectonic differentiation within ICC, with very large and basophilic neurons that were arrayed in rows in a

Fig. 4. ICS at a more frontal plane. **a:** Gallyas stains from A3.41. **b:** DARPP-32 stain from A3.50. **c:** Calbindin stain from A3.53. **d:** Cresyl violet stain from A3.38. Note the clear zone in the ICSd in the calbindin stain. Note also the more medial extension of ICS compared with the pictures shown in Figure 3. For abbreviations, see list. Scale bar = 1,000 μm in a,b,d; 500 μm in c.



dorsolateral to ventromedial orientation, as may be seen by the more structured appearance of the ICCc compared with the ICCs (Fig. 5a; see also Takahashi and Konishi, 1988). As seen in Gallyas stains, the density of the fibers seemed to reach a maximum in the ICCc with respect to the other subnuclei of the IC complex (Fig. 6a). In the frontal part of the ICC, the ICCls occupies the entire dorsoventral and mediolateral region (A3.82). In the caudal part the ICCls borders directly with the ICCms (A1.64). None of the markers labeled the ICCls-ICCms border.

DISCUSSION

We have presented a thorough analysis of the anatomical components of the barn owl's inferior colliculus and the adjacent tectal layer 15. By using seven different histochemical and immunocytochemical markers, we outlined the position, size, and staining patterns of eight structures (Fig. 11). As for the anatomy of the superficial nucleus of the inferior colliculus, we present the most detailed description to be carried out thus far. In the following paragraphs we shall set these findings into the context of earlier reports on the anatomy of the inferior colliculus of the barn owl and discuss the relationship between our data and other physiological findings. Finally, we shall compare the inferior colliculus of the owl with the homologous structures in other birds and mammals.

Anatomy of the superficial nucleus of the inferior colliculus (ICS)

The ICS nucleus was first studied by Knudsen (1983), who called it the superficial nucleus due to its position at the dorsal border of the IC complex. He differentiated a deep and a superficial part. We also observed a division of a dorsal and a ventral part. Knudsen (1983) reported that the nucleus was directly bordering the ICC and the ICX. We found that the ICS was embedded in tectal layer 15 and had no direct contact with either the ICC or the ICX. In accordance with earlier studies, we included the ICS in the nuclei of the IC. However, the separation of the ICS from the rest of the IC raises the question of whether the ICS is really part of the inferior colliculus or might belong to the intercollicular nuclei (see also Dubbeldam and den Boer-Visser, 2002). This question cannot be answered, given the nature of our study. Hodological data that were beyond the scope of this work will be needed to decide this issue. The ICS was marked in several other studies [e.g.,

Fig. 6. Gallyas-stained sections of the IC complex. **a**: Frontal section at A3.05. Insets in a delineate areas that are shown at higher magnification in b and c. ICC and the dorsomedial part of layer 15 were heavily labeled, whereas ICX and ICS could be differentiated by lower fiber density (a). Note the dorsoventral orientation of fibers in ICX (a,c). **b**: In the higher magnification of layer 15 at the ventral part of the ventricle, it becomes obvious that a line of thick fibers separates layer 15a from layer 15b (arrow). **c**: Border of ICX and ICC to the adjacent SAC (stratum album centrale) of the OT. Afferent and efferent fibers are especially evident in SAC underlying ICX (white arrowheads). **d**: Horizontal section from D 0.36. The arrow points toward the fiber tract already alluded to in c. Note that a and d are composite pictures. For abbreviations, see list. Scale bars = 1,000 μ m in a,d; 250 μ m in b,c.

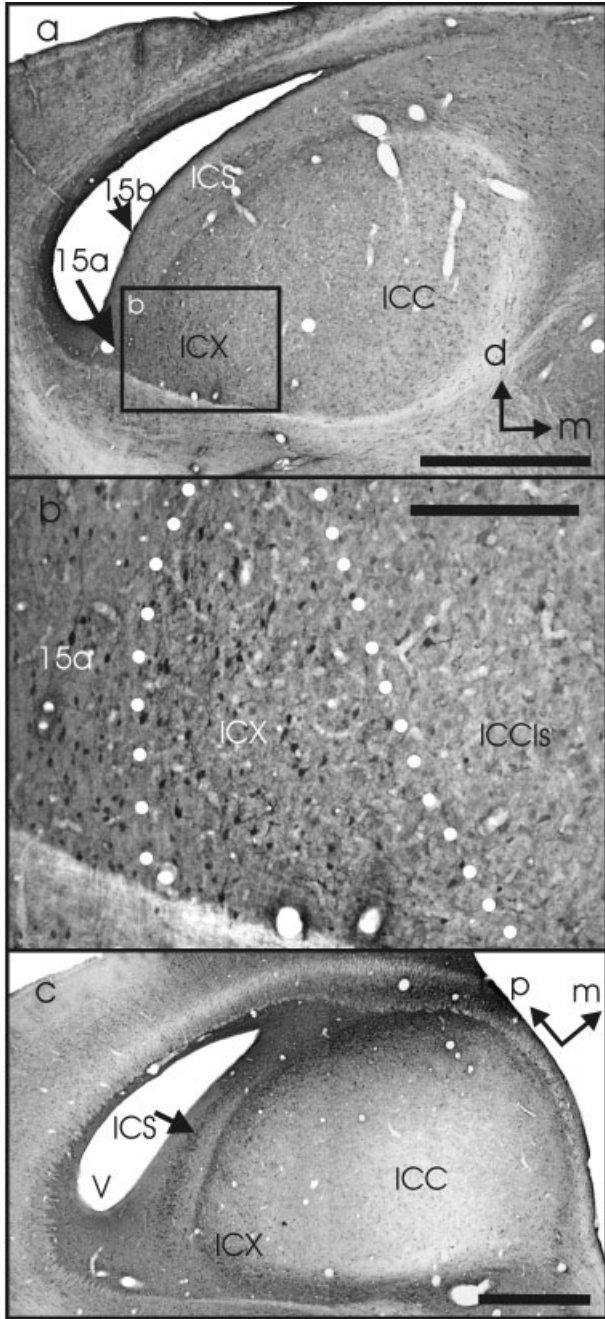


Fig. 7. Labeling with an antibody against DARPP-32. **a**: Frontal section at level A3.14. ICC displays a homogeneous staining of neuropil with several stained somata. **b**: Higher magnification demonstrates borders of more heavily stained ICX (white dots). **c**: Horizontal section of the IC complex at D 0.54. Note the clear border between ICX and 15a. Note that c is a composite picture. For abbreviations, see list. Scale bars = 500 μm in a; 250 μm in b; 1,000 μm in c.

Takahashi and Konishi, 1988; Takahashi et al., 1989; Carr et al., 1989; Levin et al., 1997 (their Fig. 9D)], although the delineation of the position and size of the ICS differed in these studies. For example, the ICS as marked by Levine et al. (1997) or Takahashi et al. (1989) is rather comparable to layer 15a of this study.

Anatomy of the ICX and the ICC in the owl

Knudsen (1983) discriminated a dorsal and a ventral subdivision in ICC but also stated that "undoubtedly more anatomically and physiologically definable subdivisions exist within the ICC." Our immunocytochemistry together with Nissl and Gallyas stains allowed the discrimination of four nuclei below and medial to layer 15a. The stainings presented here complement earlier stainings with calcium-binding protein (Takahashi et al., 1987), horseradish peroxidase and tritiated proline (Takahashi and Konishi, 1988), glutamic acid decarboxylase (Carr et al., 1989), acetylcholinesterase (Adolphs, 1993), and AMPA receptor subunits GluR1–4 (Levin et al., 1997) that have identified similar structures.

The ICX, the most lateral part of the IC, is clearly separable from the tectal layer 15a in most stains. More specifically, this border was the only one marked with the antibody against TH. The border between the ICX and the ICC is not as clear. In our study, this border was best visible in DARPP-32 and GABA_{AB} stains. Thus these two stains are good markers for establishing the boundary between the ICC and the ICX. Interestingly, the border between the ICX and the ICCls is also more continuous than sharp in tuning properties like width of frequency tuning, tuning to interaural time difference, and tuning to interaural level difference (Mazer, 1998).

In the ICC, the ICCc as marked by calbindin and calretinin is the most well-defined structure. The ICCc separates the medial from the lateral shell. Caudally, the ICCls and the ICCms share a common border. This border has only been defined physiologically so far. The dorsoventral division as reported by Knudsen (1983) could not be seen in our stains.

Borders between 15a, ICX, and ICCls and their relation to developmental plasticity

In barn owl development the visual system instructs the auditory system by changing the map of auditory space (Brainard and Knudsen, 1993). Candidate correlates for the instructive signal have recently been found (Luksch et al., 2000; Hyde and Knudsen, 2000). The available data point toward the ICX as the site of adaptive changes. No influence of the tectal signal on tuning in the ICC was observed (Brainard and Knudsen, 1993; Feldman and Knudsen, 1997; Gold and Knudsen, 2000; deBello et al., 2001). Such a conclusion depends on a clear anatomical separation of layer 15a, the ICX, and the ICCls. Although Feldman and Knudsen (1997) carefully separate the ICX from 15a, Gold and Knudsen (2000) as well as Brainard

Fig. 8. Staining with antibodies against calbindin (a,c,e,g) and calretinin (b,d,f,h). **a**: Frontal section at A3.17. **b**: Frontal section at level A3.08. Insets in a and b delineate areas that are shown with higher magnification in c–f. **c**: ICX borders with lamina 15a and ICCls in calbindin stains. **d**: Same borders with calretinin stain. **e**: ICCc borders with ICCls and ICCms in calbindin stain. **f**: ICCc borders with ICCls and ICCms in calretinin stain. **g**: Horizontal section stained with an antibody against calbindin at D0.33. **h**: Horizontal section stained with antibody against calretinin from D 0.45. Note that the ICCc is clearly delineated by darker staining and that both horizontal sections are at a level below ICS. Abbreviations are explained in the list of abbreviations. Note that g and h are composite pictures. For abbreviations, see list. Scale bars = 1,000 μm in a,b,g,h; 250 μm in c–f.

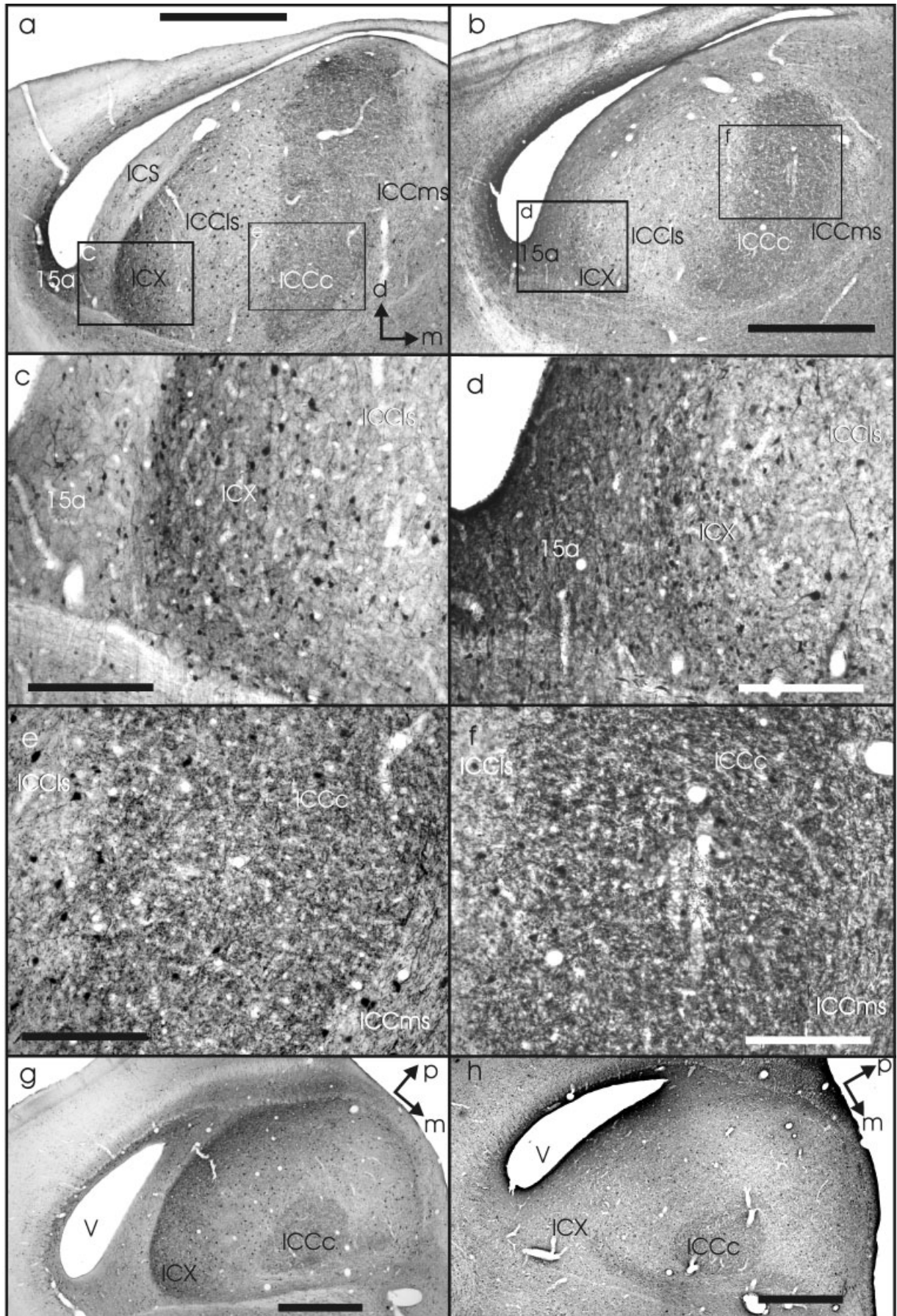


Figure 8

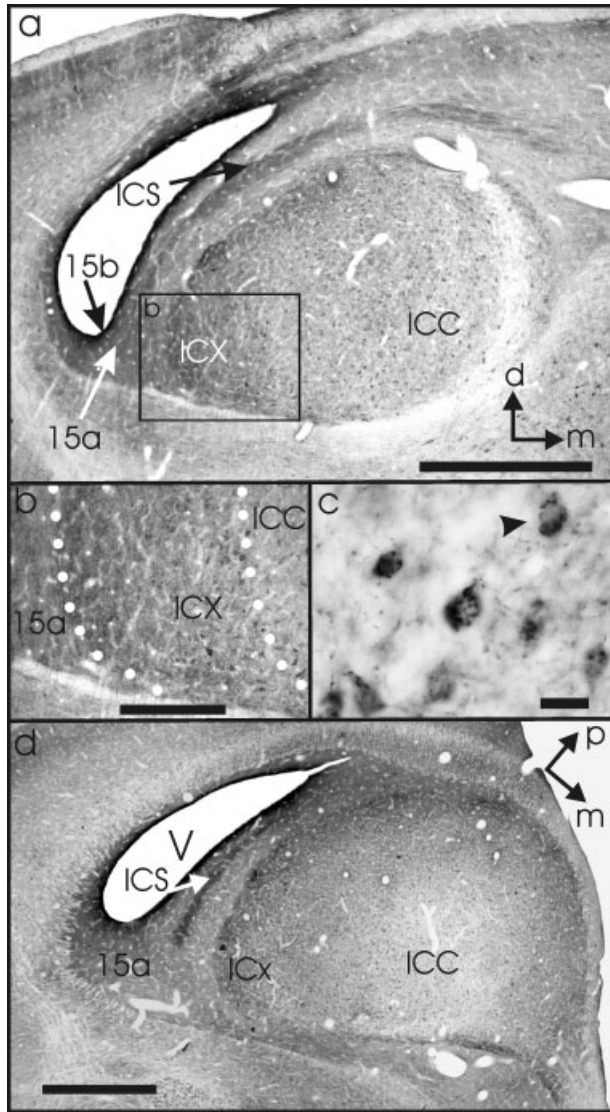


Fig. 9. IC complex stained with an antibody against $GABA_{A\beta}$. **a**: Frontal section at level A3.35. Inset delineates the area that is shown at higher magnification in **b**. **b**: ICX can be delineated by intense staining of the neuropil. **c**: In ICC the staining of the neuropil was less intense than in ICX. However, single cells were surrounded by stained endbulb-like structures (**c**). **d**: Horizontal section at D 0.84. For abbreviations, see list. Note that **d** is a composite picture. Scale bars = 1,000 μm in **a,d**; **b**, 250 μm in **b**; 20 μm in **c**.

and Knudsen (1993) seem to include layer 15a within their "ICX." This raises the possibility that physiological properties of 15a cells and the ICX cells were mixed in some cases. A similar difficulty exists with respect to the border between the ICCLs and the ICX. Our measurements based on anatomical markers suggest a distance of some 600–700 μm between the lateral edge of the core and the ICCLs-ICX border (Fig. 12), very close to the value of 600 μm used by Feldman and Knudsen (1997) and deBello et al. (2001). On the other hand, Brainard and Knudsen (1993) divided the ICX into a medial and a lateral part, with the medial part extending up to 750 μm lateral to the

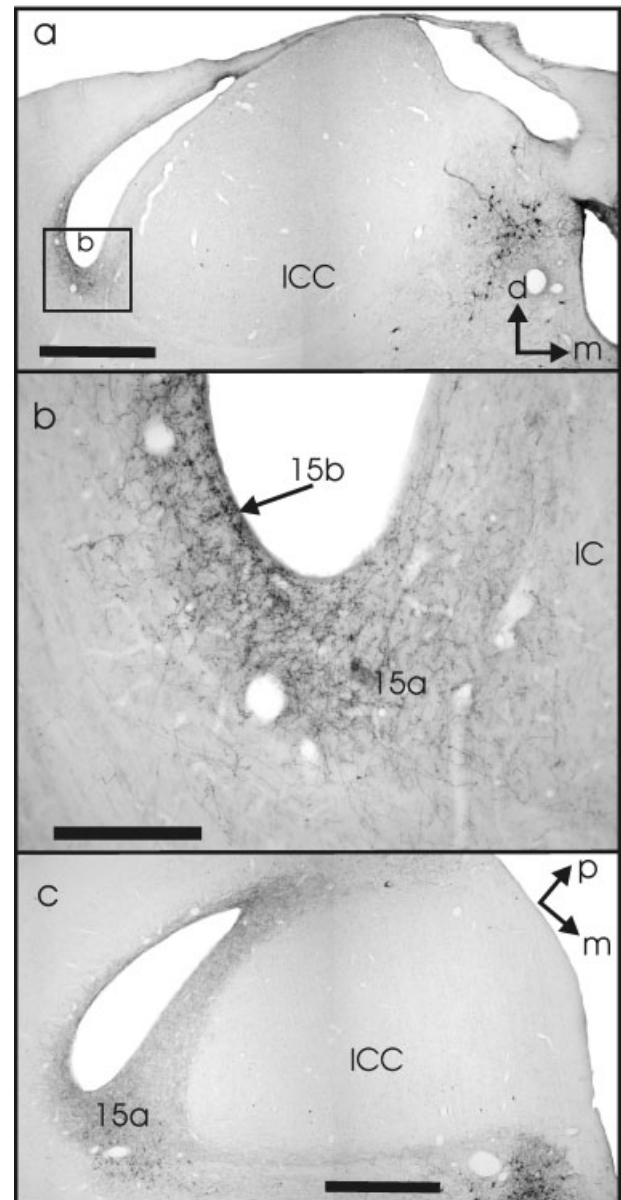


Fig. 10. TH-stained sections. **a**: Frontal section at level A2.21. Inset delineates area of higher magnification shown in **b**. Note that immunoreactive label is restricted to ventral layer 15. **b**: Horizontal section at D 0.6. Note that **a** and **c** are composite pictures. For abbreviations, see list. Scale bars = 1,000 μm in **a,b**; 200 μm in **c**.

core border. In the medial part no or only small shifts of auditory-receptive fields in response to shifts of the visual field were observed. The measurements presented here suggest that the medial part of the ICX as outlined by Brainard and Knudsen (1993) may—at least in part—belong to the ICCLs. We therefore suggest the following protocol to avoid misinterpretations: a combination of calbindin (to mark the ICX-15a border and to mark the ICCLs), DARPP-32 (or $GABA_{A\beta}$; to mark the ICX-ICCLs border), and cresyl violet stains (to mark the stratum griseum et fibrosum superficiale in the optic tectum as a

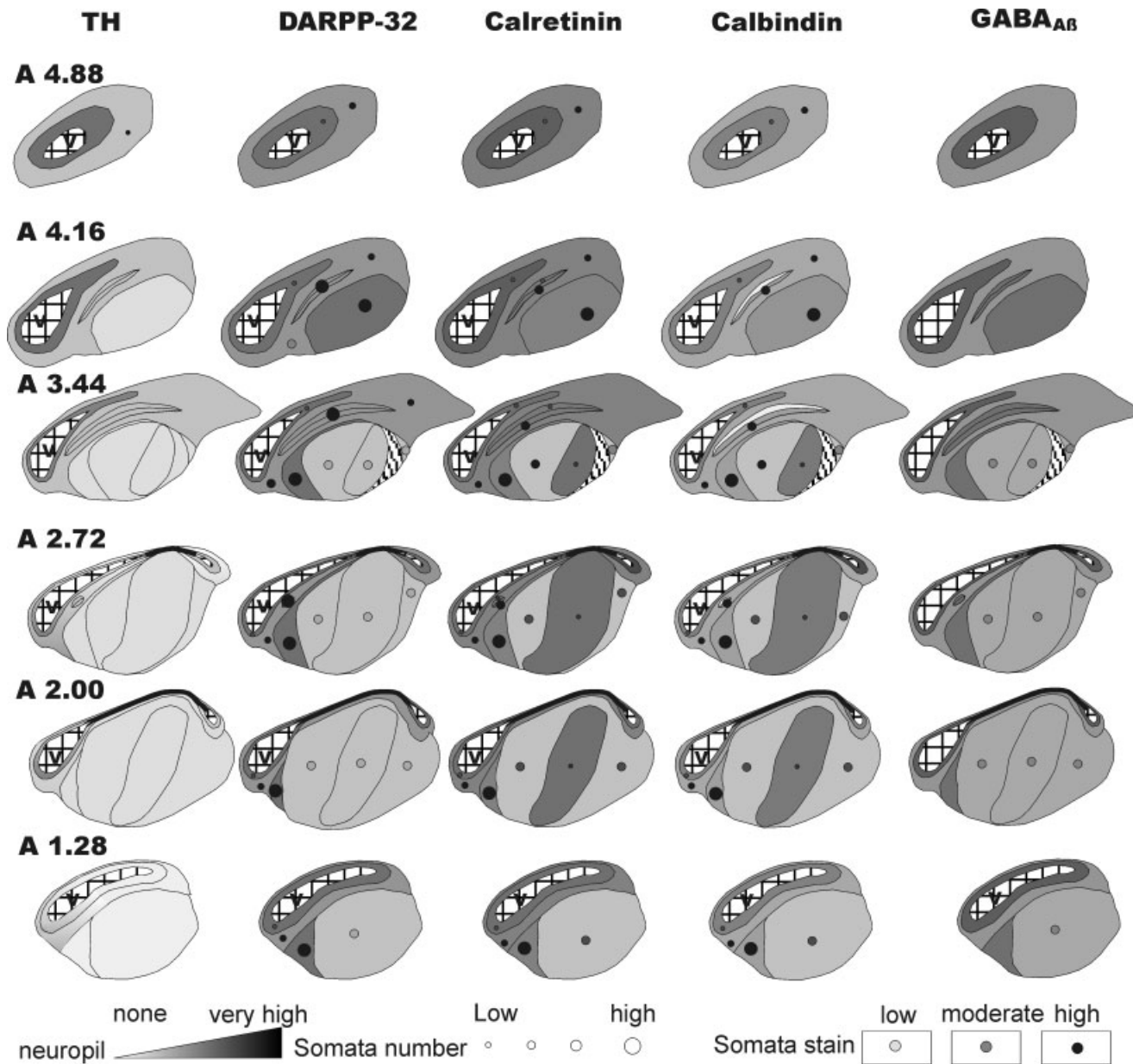


Fig. 11. Schematic overview of immunochemically labeled frontal sections through the IC complex depicting labeled perikarya (dots) and neuropil. Density of the number of labeled somata is represented by circle size. Density of somata staining is represented by three

shadings, as indicated in the figures. Density of neuropil staining is indicated by a black/white gradient. Note that due to the categorization in the schemes not all the nuances seen in the pictures can be documented.

reference structure). For the delineation of 15a from the ICX, TH would also be suitable, although it is less powerful than than calbindin as it does not stain the IC at all.

Relation of owl IC to the IC in other birds and in mammals

After the early cellular work by Ramón y Cajal (1891), Karten (1967) provided a description of the diencephalic projections of the pigeon IC. He was also the first to use the term “inferior colliculus” for this structure. Puelles et al. (1994) took advantage of modern immunocytochemis-

try and histochemistry to revise the organization of the IC in the chick. The IC was divided into 10 subnuclei in total by Puelles et al. (1994). Their toral nucleus, equivalent to the IC referred to here, consisted of three major subnuclei.

The periventricular lamina of Puelles et al. (1994), which was divided into a basophilic core lamina of compact neurons and a deep and superficial cell-sparse shell region, bears a resemblance to the four dorsal laminae in our data (layers 15a and 15b, ICSD, ICSDv). Indeed, Puelles et al. (1994) drew equivalence between the core area of the periventricular lamina and the ICS. However, they did not

- deBello WM, Feldman DE, Knudsen EI. 2001. Adaptive axonal remodeling of the midbrain auditory space map. *J Neurosci* 21:3161–3174.
- Dubbeldam JL, den Boer-Visser AM. 2002. The central mesencephalic grey in birds: Nucleus intercollicularis and substantia grisea centralis. *Brain Res Bull* 57:349–352.
- Cowan WM, Adamson L, Powell TPS. 1961. An experimental study of the avian visual system. *J Anat (Lond)* 95:545–563.
- Dezso A, Schwarz DW, Schwarz IE. 1993. A survey of the auditory midbrain, thalamus and forebrain in the chicken (*Gallus domesticus*) with cytochrome oxidase histochemistry. *J Otolaryngol* 22:391–396.
- Durstewitz D, Kröner S, Hemmings HC Jr, Greengard P, Güntürkün, O. 1998. The dopaminergic innervation of the pigeon telencephalon: distribution of DARPP-32 and cooccurrence with glutamate decarboxylase and tyrosine hydroxylase, *Neuroscience* 83:763–779.
- Feldman DE, Knudsen EI. 1997. An anatomical basis for visual calibration of the auditory space map in the barn owl's midbrain. *J Neurosci* 17:6820–6837.
- Gold JI, Knudsen EI. 2000. A site of auditory experience-dependent plasticity in the neural representation of auditory space in the barn owl's inferior colliculus. *J Neurosci* 20:3469–3486.
- Hemmings HC, Walaas SI, Ouimet CC, Greengard P. 1987. Dopaminergic regulation of protein phosphorylation in the striatum: DARPP-32. *Trends Neurosci* 10:377–383.
- Hess DT, Merker BH. 1983. Technical modifications of Gallyas' silver stain for myelin. *J Neurosci Methods* 8:95–97.
- Hyde PS, Knudsen EI. 2000. Topographic projection from the optic tectum to the auditory space map in the inferior colliculus of the barn owl. *J Comp Neurol* 421:146–160.
- Karten HJ. 1967. The organization of the ascending auditory pathway in the pigeon (*Columba livia*). I. Diencephalic projections of the inferior colliculus (nucleus mesencephali lateralis, pars dorsalis). *Brain Res* 6:409–427.
- Knudsen EI. 1983. Subdivisions of the inferior colliculus in the barn owl (*Tyto alba*). *J Comp Neurol* 218:174–186.
- Knudsen EI, Knudsen PF. 1983. Space-mapped auditory projections from the inferior colliculus to the optic tectum in the barn owl. *J Comp Neurol* 218:187–196.
- Knudsen EI, Konishi M. 1978. Space and frequency are represented separately in auditory midbrain of the owl. *J Neurophysiol* 41:870–884.
- Kubke F, Gauger B, Basu L, Wagner H, Carr CE. 1999. Development of calretinin immunoreactivity in the brainstem auditory nuclei of the barn owl (*Tyto alba*). *J Comp Neurol* 415:189–203.
- Levin MD, Kubke MF, Schneider M, Wenthold R, Carr CE. 1997. Localization of AMPA-selective glutamate receptors in the auditory brainstem of the barn owl. *J Comp Neurol* 378:239–253.
- Luksch H, Gauger B, Wagner H. 2000. An anatomical correlate for a visual instructional signal to the auditory system. *J Neurosci* 20:1–4.
- Mazer JA. 1998. How the owl resolves auditory coding ambiguity. *Proc Natl Acad Sci U S A* 95:10932–10937.
- Morest DK, Oliver DL. 1984. The neuronal architecture of the inferior colliculus in the cat: defining the functional anatomy of the auditory midbrain. *J Comp Neurol* 222:209–236.
- Oliver DL, Shneiderman A. 1991. The anatomy of the inferior colliculus: a cellular basis for integration of monaural and binaural information. In: Altschuler RA, Bobbin RP, Clopton BM, Hoffman DW, editors. *Neurobiology of hearing: the central auditory system*. New York: Raven Press. p 195–222.
- Ouimet CC, Miller PE, Hemmings HV, Walaas SI, Greengard P. 1984. DARPP-32, a dopamine- and adenosine 3':5'-monophosphate-regulated phosphoprotein enriched in dopamine-innervated brain regions, III. Immunocytochemical localization. *J Neurosci* 4:111–124.
- Puelles L, Robles C, Martinez-de-la-Torre M, Martinez S. 1994. New subdivision schema for the avian torus semicircularis: neurochemical maps in the chick. *J Comp Neurol* 340:98–125.
- Ramón y Cajal S. 1891. Sur la fine structure du lobe optique des oiseaux et sur l'origine réelle des nerfs optique. *Int Mschr Anat Physiol* B8:337–366.
- Rockel AJ, Jones EG. 1973a. Neural organization of inferior colliculus of adult cat. I. Central nucleus. *J Comp Neurol* 147:11–60.
- Rockel AJ, Jones EG. 1973b. Neural organization of inferior colliculus of adult cat. II. The pericentral nucleus. *J Comp Neurol* 149:301–334.
- Schwaller B, Buchwald P, Blumcke I, Celio MR, Hunziker W. 1993. Characterization of a polyclonal antiserum against the purified human recombinant calcium binding protein calretinin. *Cell Calcium* 14:639–638.
- Takahashi TT, Konishi M. 1988. Projections of the cochlear nuclei and nucleus laminaris to the inferior colliculus of the barn owl. *J Comp Neurol* 274:190–211.
- Takahashi TT, Carr CE, Brecha N, Konishi M. 1987. Calcium binding protein-like immunoreactivity labels the terminal field of nucleus laminaris of the barn owl. *J Neurosci* 7:1843–1856.
- Takahashi TT, Wagner H, Konishi M. 1989. Role of commissural projections in the representation of bilateral auditory space in the barn owl's inferior colliculus. *J Comp Neurol* 281:545–554.
- Wild M. 1995. Convergence of somatosensory and auditory projections in the avian torus semicircularis, including the central auditory nucleus. *J Comp Neurol* 358:465–486.